1 Science Program

The Proposed Research Plan

The measurement of cosmic acceleration – the increasingly rapid expansion of the Universe over time – was awarded the Nobel Prize in Physics in 2011. This acceleration either signals that a gravitationally repulsive dark energy dominates the energy density of the Universe today or that Einstein's General Relativity does not correctly describe gravity on cosmological scales. The impact of this discovery on fundamental physics and astrophysics is revolutionary, and decoding the physics of cosmic acceleration requires new, higher-quality measurements of the expansion rate of the Universe as a function of time.

Measuring the Expansion History of the Universe

Nature has provided a standard ruler with which to measure the Universe's expansion history: the "baryon acoustic oscillation" (BAO) length scale (Seo & Eisenstein, 2003, 2007). Acoustic waves propagated through the primordial plasma in the early Universe for a fixed amount of time: 379,000 years, until the plasma cooled and became neutral gas (mostly hydrogen). The distance these waves travelled has been precisely measured in the Cosmic Microwave Background (CMB) radiation (Komatsu et al., 2011). These waves imparted slight baryonic over-densities on the BAO scale which are imprinted in the large-scale distribution of matter in the Universe. By measuring cosmic structure as a function of time, we can deduce the apparent size of the BAO scale as a function of cosmic epoch and hence the expansion history of the Universe.

The signature of BAO was first detected in "nearby" cosmic structure, at redshift $z = 0.35$, using galaxies as tracers (Eisenstein et al., 2005). More recently, measurements of the BAO scale at redshifts up to $z = 0.8$ have been made by observing the distribution of optically-detected galaxies (2dFGRS (Percival et al., 2007), 6dFGS (Beutler et al., 2011), SDSS (Padmanabhan et al., 2012), BOSS (Anderson et al., 2012), WiggleZ (Blake et al., 2011)).

In a recent Nature paper (Chang et al., 2010), a new way to map the three-dimensional distribution of matter, "hydrogen intensity-mapping", was successfully demonstrated. The technique uses observations of redshifted 21 cm emission from the hyperfine transition of neutral hydrogen to trace the distribution of hydrogen gas, and thus matter, in the Universe. Hydrogen intensity-mapping allows the apparent angular and radial BAO scale to be measured through cosmic history without the expensive and time-consuming step of resolving individual galaxies.

Though hydrogen intensity-mapping was first demonstrated using a conventional radio telescope, a dedicated instrument is needed to make a measurement of cosmic acceleration with the sensitivity needed to test models.

CHIME is an ambitious project to use 21cm radiation to map a significant fraction of the the Hubble volume in the search for dark energy. We quantify five milestones on this path: the CHIME pathfinder will sit in the range 2-4, while the full instrument aims for the last.

1. The first is being able to see any cosmological 21cm structure in the radio maps. This has already been achieved in cross correlation with optical galaxy surveys using the GBT. It requires a reduction of foregrounds by at least a factor of 100 to reduce the noise from the foregrounds.

2. The second stage is to measure the 21cm power spectrum itself. The pathfinder should easily achieve this stage in a few weeks of observing, even for pessimistic assumptions.

3. The third stage is detection of BAO in the large scale distribution of 21cm structure, and is the nominal science goal of the pathfinder.

4. The fourth stage is to measure BAO better than any existing or contemporary survey. In the optimistic scenario, the pathfinder will reach this stage after 2 years integration.

5. The fifth stage is to approach the cosmic variance limit and map the Hubble Volume. Planck is approaching this stage for the CMB. CHIME aims to tackle this grand goal for 21cm in the epoch of dark energy domination. The design parameters are drawn to aim at this goal.

2 CHIME Design Parameters

Frequency coverage - An effective measurement of dark energy requires probing the epoch just before and after dark energy drives the universe from decelerating to accelerating expansion. This transition occurs at a redshift slightly above $z = 1$. (21 cm line radiation emitted at $z = 1$ has an observed frequency of 710 MHz today.) The frequency coverage is chosen to avoid terrestrial foregrounds while maximizing sensitivity to dark energy; the latter is demonstrated in Figure 1, which shows the relative improvement CHIME provides to the Dark Energy Task Force (DETF) Figure of Merit (FoM) (Albrecht et al., 2006).

By observing over the frequency range 400-800 MHz, CHIME will map hydrogen emission over the redshift range $0.8 \leq z \leq 2.5$. This band covers the important epoch in cosmic history when the expansion transitioned from decelerating to accelerating (Riess et al., 2004), while avoiding interference from cellular telephone transmitters and without overlapping low-redshift galaxy surveys. It also covers the "optical redshift desert" $1.3 \lesssim z \lesssim 2.5$, which is difficult to access from the ground due to a lack of suitable emission-lines in the observable frequency range.

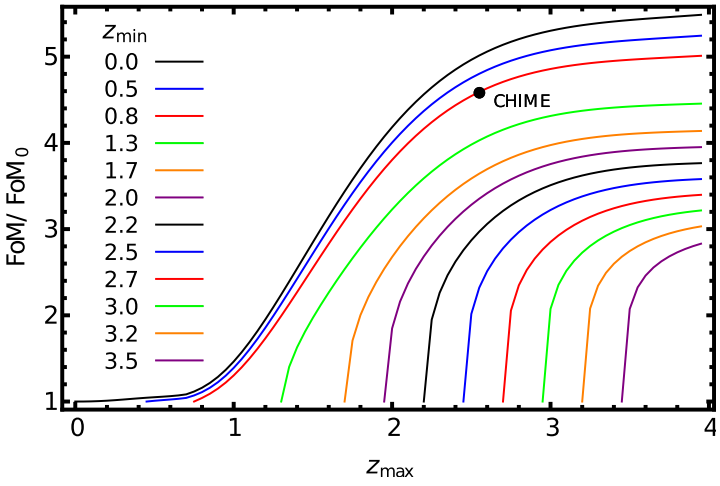

Figure 1: CHIME's sensitivity to dark energy parameters depends on the redshift range surveyed. The panel shows the relative improvement in the DETF Figure of Merit (FoM) over near-term measurements (Planck+DETF StageII+BOSS) as a function of survey redshift range. Each curve gives the improvement CHIME brings to FOM for a given $z_{\rm min}$ and $z_{\rm max}$. The improvement is limited above $z_{\rm max} \approx 2.5$, and the BOSS data at $z < 0.8$ limits the benefit of CHIME observing $z < 0.8$. The selected CHIME band is indicated.

Angular resolution - To constrain cosmological models to an interesting level, the sky maps should have sufficient spatial resolution to resolve the smallest useful features while surveying a volume that is large enough to observe many independent BAO-scale fluctuations.

The design is driven by the lowest frequency, i.e. highest redshift. At 400 MHz, this is $z = 2.5$, where the resolution is the worst, cosmic structures are the smallest, sensitivity and foregrounds are most challenging. A baseline of 80m corresponds to $l \sim 700$, transverse wavenumber $k \sim 0.16h$/Mpc, which is well matched to the third BAO peak. The minimum spacing is 20m, driven by the lowest observed redshift $z = 0.8$, $l = 330$, $k = 0.16$.

Features smaller than ∼10 Mpc (∼30 million light-years) today have been significantly affected by non-linear gravitational interactions over time and provide little direct information about their primordial origin. Using the angular size-distance relation for ΛCDM, an effective aperture of ∼100 m is able to resolve structure at ∼10 Mpc. Table 1 gives more precise values for CHIME's spatial resolution as a function of redshift.

Frequency resolution - CHIME maps hydrogen intensity as a function of redshift (frequency) along the line of sight. If we insist that its radial distance resolution matches its transverse distance resolution provided by the angular response, a frequency resolution of $2.0 - 5.1$ MHz is required in

the redshift range $0.8 \leq z \leq 2.5$, as indicated in Table 1. In practice, CHIME will have a resolution of ~ 1 MHz at all frequencies.

z	$f_{\rm obs}$	CHIME resolution			BAO scale		
		co-moving	Δz	Δf	co-moving	Δz	Δf
	MHz	Mpc		MHz	Mpc		MHz
0.8	789	12.95	0.0046	2.02	150	0.054	23.0
1.	710	17.10	0.0069	2.44	150	0.060	20.6
2.	473	40.56	0.027	4.25	150	0.10	15.3
2.5	406	53.35	0.044	5.09	150	0.12	13.5

Table 1: Summary of CHIME angular and frequency resolution. The first column is the redshift of observation, the second is the observed frequency of 21 cm radiation emitted at that redshift. The next three columns give the distance increment corresponding to CHIME's angular resolution at each redshift: as a co-moving distance, as a redshift increment, and as a frequency increment to 21cm radiation. The last three columns give the same information for the co-moving BAO scale at each redshift, showing that CHIME resolves the BAO scale over the full redshift range.

Frequency contamination - The 21 cm hydrogen line is the dominant spectral feature at frequencies less than 1420 MHz and it is an isolated transition. This allows us to interpret the apparent frequency of a source directly in terms of its redshift, without the elaborate spectral fitting required for typical optical redshift measurements. The strongest potential line contaminant is the OH maser line, which has been shown by modelling to be insignificant (Gong et al., 2011).

Physical design - A drift scan telescope with no moving parts is very stable, which is an important consideration in the presence of very bright foregrounds. A cylinder telescope achieves a full sky view with no moving parts, while retaining substantial collecting area. The full sky rotation allows a computationally tractable solution of the wide field imaging problem, and polarization leakage calibration.

Sky coverage - Conceptually, the BAO scale is inferred from CHIME data by measuring the power spectrum of fluctuations, $P(k)$, in the three-dimensional map and fitting $P(k)$ for the BAO scale (see Figure 3). In the absence of noise, the power spectrum sensitivity is proportional to the number of independent modes measured, which in turn is proportional to the volume of space observed. CHIME is able to usefully observe half the sky from its site in Penticton, BC.The baseline plan is for CHIME to observe the entire sky visible from Penticton and to reject some portion of the data near the Galactic plane due to excessive foreground contamination .

Nominal Design The fiducial design parameters are presented in Table 2, and a cartoon drawing of the final instrument is shown in Figure 2.

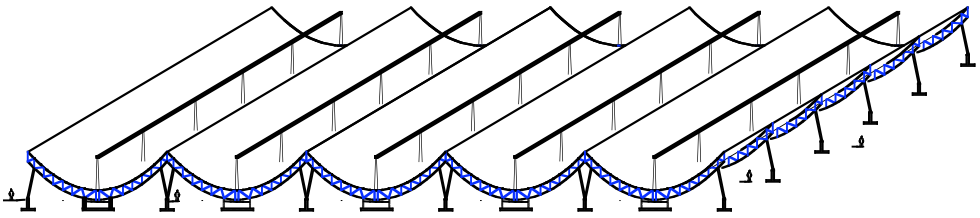

Figure 2: The CHIME telescope consists of five parabolic, cylindrical reflectors and associated radio receivers and correlators. The structure is 100m × 100m. Note the people in the figure, for scale. The telescope has no moving parts, and maps half of the sky every day.

Observing frequency	800 to 400 MHz
Observing wavelength	37 to 75 cm
Redshift	$z \approx 0.8$ to 2.5
System noise temperature	$\sim$ 50K
Beam size	0.26° to 0.52°
Field of view, N-S	180°
Field of view, E-W	1.3° to 2.5°
Number of cylinders	5
Cylinder size	100 m × 20 m
Collecting area	10,000 m^2
Dual-polarization antenna spacing	$\sim$31 cm
Number of antennas per cylinder	256
Bandwidth of channeled outputs	$\sim$ 1 MHz

Table 2: Fiducial CHIME Design parameters.

Performance Forecasts

A measurement of the BAO scale in the CMB at early times combined with BAO measurements from the large-scale structure at late times provides a very robust probe of expansion history, and hence dark energy models. Assuming the telescope described above, we forecast CHIME's sensitivity to measurements of the power spectrum, $P(k)$, and derive from that CHIME's sensitivity to the distance-redshift relation, D_V/s, and to the dark energy equation of state parameters w_0 and w_a. The latter parameterize an evolving equation of state: $w(a) = w_0 + w_a(1-a)$, where $a = 1/(1+z)$ is the scale factor.

CHIME's basic power spectrum sensitivity is shown in Figure 3, where a smooth "zero-baryon" $P_{\rm smooth}(k)$ has been divided out to highlight the oscillations induced by BAO in the large-scale structure.

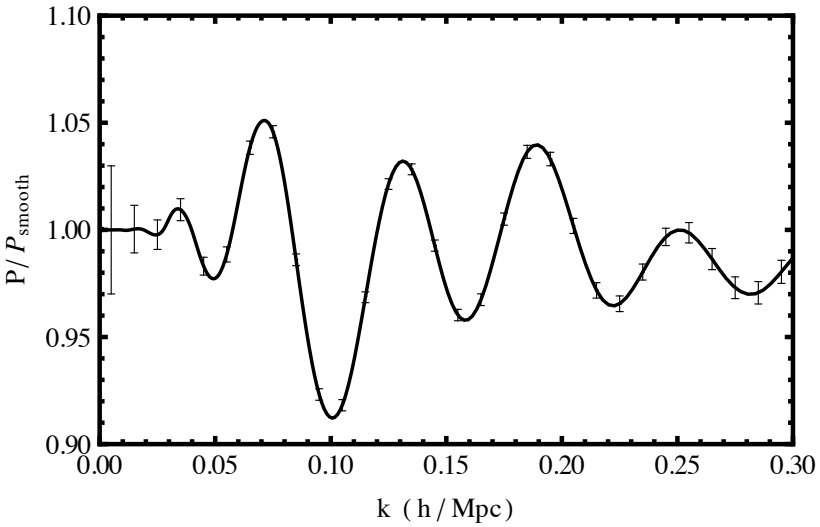

Figure 3: *Solid curve* - The ratio of ΛCDM power spectra, $P(k)$, with and without Baryon Acoustic Oscillations. *Points with errors* - the CHIME sensitivity forecast using the formalism of Seo et al. (2010). We assume a 2-year survey and project the data to a single effective redshift. CHIME's physical size is chosen to resolve this structure (Table 1).

Given radial and tangential estimates of the BAO scale from CHIME data, we use the Seo et al. (2010) formalism to forecast uncertainties in the effective distance measure $D_V(z)$ (Eisenstein et al., 2005) in Figure 4. CHIME will extend the range of BAO-based distance measurements well past existing galaxy survey measurements, into the key – and as-yet unmeasured – redshift range of $0.8 \leq z \leq 2.5$, the epoch when the expansion transitioned from decelerating to accelerating.

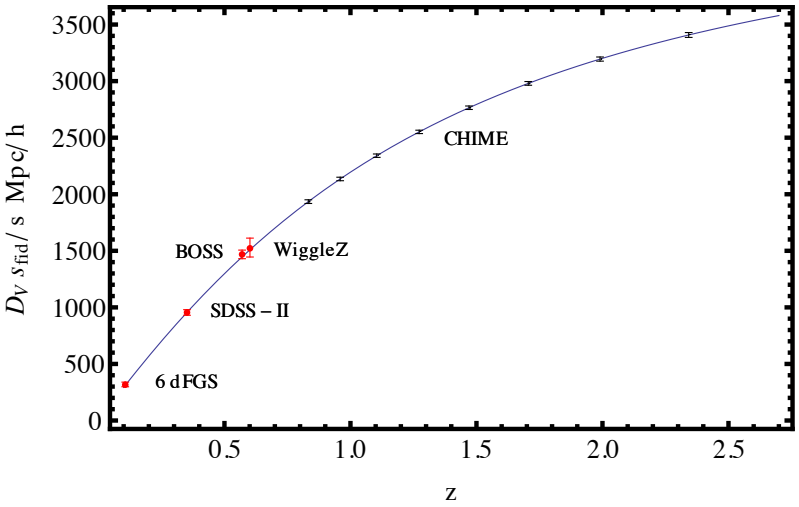

Figure 4: BAO-based distance measurements. *Solid curve* - Effective distance vs redshift for standard ΛCDM. *Red points* - existing measurements left-to-right: 6dFGS (Beutler et al., 2011), SDSS (Padmanabhan et al., 2012), BOSS (Anderson et al., 2012), and WiggleZ (Blake et al., 2011). *Grey points with errors* - CHIME forecast using the (Seo et al., 2010) formalism, assuming a 2-year survey.

CHIME's measurements of the BAO scale can be combined with those from lower and higher

redshift, using galaxy redshift surveys and CMB data, respectively, to yield tight constraints on the dark energy equation of state parameters w_0 and w_a (Figure 5).

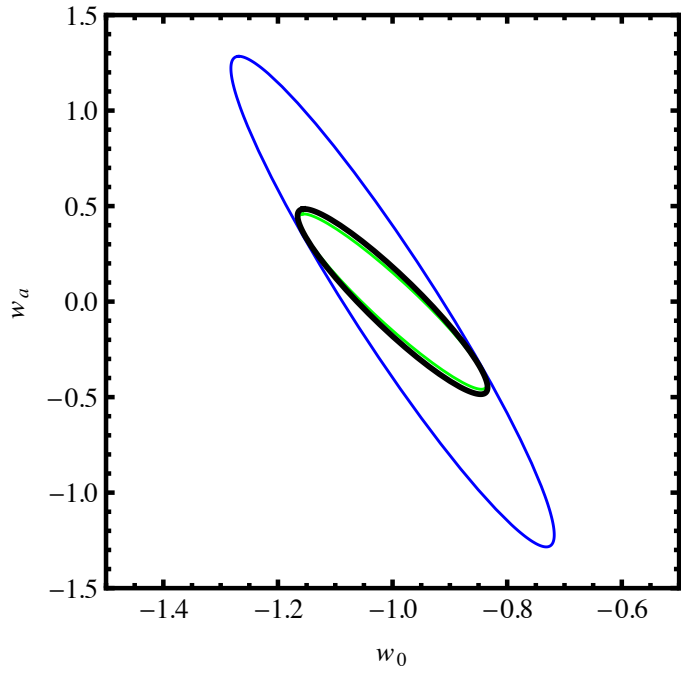

Figure 5: Projected 2σ constraints on the dark energy parameters w_0 and w_a. *blue* - constraints from Planck and DETF Stage II experiments;
green - Planck+StageII plus cosmic-variance-limited BAO measurements from the proposed EUCLID satellite or BigBOSS project;
black: Planck+StageII plus CHIME BAO constraints, calculated for a 2 year survey, using the formalism in (Seo et al., 2010).

References

Albrecht, A., et al. 2006, ArXiv e-prints, arXiv:astro-ph/0609591

Anderson, L., et al. 2012, ArXiv e-prints, 1203.6594

Beutler, F., et al. 2011, MNRAS, 416, 3017

Blake, C., et al. 2011, MNRAS, 415, 2892

Chang, T.-C., Pen, U.-L., Bandura, K., & Peterson, J. B. 2010, ArXiv e-prints, 1007.3709

Eisenstein, D. J., et al. 2005, ApJ, 633, 560

Gong, Y., Chen, X., Silva, M., Cooray, A., & Santos, M. G. 2011, ApJ, 740, L20

Komatsu, E., et al. 2011, ApJS, 192, 18

Padmanabhan, N., Xu, X., Eisenstein, D. J., Scalzo, R., Cuesta, A. J., Mehta, K. T., & Kazin, E. 2012, ArXiv e-prints, 1202.0090

Percival, W. J., Cole, S., Eisenstein, D. J., Nichol, R. C., Peacock, J. A., Pope, A. C., & Szalay, A. S. 2007, MNRAS, 381, 1053

Riess, A. G., et al. 2004, ApJ, 607, 665

Seo, H.-J., Dodelson, S., Marriner, J., Mcginnis, D., Stebbins, A., Stoughton, C., & Vallinotto, A. 2010, ApJ, 721, 164

Seo, H.-J., & Eisenstein, D. J. 2003, ApJ, 598, 720

——. 2007, ApJ, 665, 14